An efficient and general approach for implementing thermodynamic phase-equilibria information in geophysical and geodynamic studies

Juan Carlos Afonso,[1] Sergio Zlotnik,[2] Pedro Diez,[2]

Abstract. We present a flexible, general and efficient approach for implementing thermodynamic phase equilibria information (in the form of sets of physical parameters) into geophysical and geodynamic studies. The approach is based on multi-dimensional decomposition methods, which transform the original multi-dimensional discrete information into a separated representation that contains significantly less terms, thus drastically reducing the amount of information to be stored in memory during a numerical simulation or geophysical inversion. Accordingly, the amount and resolution of the thermodynamic information that can be used in a simulation or inversion increases substantially. In addition, the method is independent of the actual software used to obtain the primary thermodynamic information, and therefore it can be used in conjunction with any thermodynamic modeling program and/or database. Also, the errors associated with the decomposition procedure are readily controlled by the user, depending on her/his actual needs (e.g. preliminary runs vs full resolution runs). We illustrate the benefits, generality and applicability of our approach with several examples of practical interest for both geodynamic modeling and geophysical inversion/modeling. Our results demonstrate that the proposed method is a competitive and attractive candidate for implementing thermodynamic constraints into a broad range of geophysical and geodynamic studies. MATLAB implementations of the method and examples can be downloaded from [link].

1. Introduction

Phase equilibria calculations of crustal and mantle rocks represent one of the best sources of physical parameters (e.g. bulk density, heat capacity, elastic moduli, thermal expansion, etc) needed in both geophysical inversions and geodynamic simulations [e.g. Sobolev and Babeyko, 1994; 2005; Connolly and Kerrick, 2002; Gerya et al., 2001; 2006; Khan et al., 2006; 2011; Kuskov and Konrod, 2006; Stixrude and Lithgow-Bertelloni, 2005; Yamato et al., 2007; Xu et al., 2008; Herbert et al.; 2009; Cammarano et al., 2009; Tirone et al., 2009; Nakagawa et al., 2010; Afonso and Zlotnik, 2011; Afonso et al., 2008; 2013a,b; Davies et al., 2012; Kuskov et al., 2014, among many others]. Arguably, the main advantage of such methods over other common approaches is that they provide complete sets of thermodynamically- and internally-consistent physical parameters, therefore minimizing inconsistencies related to the use of independent mineral physics parameters "hand-picked" by non-specialists and obtained by different methods/laboratories. Parameters from thermodynamic phase equilibria calculations also explicitly consider effects of modal composition (i.e. mineral volume fractions) and mineral composition (by treating minerals as solid-solutions) as a function of pressure, temperature and composition (P-T-C), complex solid-solid mineral phase transitions (and their associated entropy and latent heat changes), hydration effects/state, and in some cases, melting. Due to the

abovementioned advantages, there has been an increasing interest in the use of thermodynamic/phase equilibria information within the geophysical and geodynamic community (see references above).

From the practical point of view, the actual implementation of such methods into geodynamic simulations or geophysical inversions is of critical importance. Traditionally, there has been two major approaches. The most popular one is the use of pre-computed property tables for specific lithologies (i.e. bulk compositions) discretized in pressure and temperature space. A third dimension (e.g. water content) can also be included to obtain a discretized cube of T-P-H_2O [e.g. Rupke et al., 2004; Nikolaeva et al., 2009; Afonso and Zlotnik, 2011]. Thus, when the size and number of tables is relatively small, the physical parameters of interest can be stored in memory as functions of e.g. P-T and retrieved (via an appropriate search algorithm) very efficiently during the course of the simulation/inversion. This approach is commonly referred to as the "static approach", and has been widely used in both geophysical and geodynamic studies [e.g. Petrini et al., 2001; Gerya et al., 2001; Rupke et al., 2004; Yamato et al., 2007; Cammarano et al., 2009; 2011; Nakagawa et al., 2010; Afonso and Zlotnik, 2011; Vozar et al., 2014]. However, the practicality of the static approach is extremely dependent on the number of tables, the dimensions of interest, and the discretization of these dimensions (i.e. number of nodes per dimension). As such, it is particularly sensitive to the so-called "curse of dimensionality", as the number of parameters to be stored in memory grow exponentially with dimension. When the number of materials or lithologies is relatively large, and for any useful discretization step of the individual axes (e.g. ΔT, ΔP, ΔF, etc), the static approach can quickly become impractical.

Alternatively, one could solve the thermodynamic equilibrium problem "on the fly", thus circumventing the need for discretized pre-computed tables; the equilibrium assemblage and associated physical parameters are computed for the exact T-P-C conditions as needed by the simulation/inversion

---

[1]CCFS, Department of Earth and Planetary Sciences, Macquarie University, North Ryde, Sydney, 2109 NSW, Australia
[2]Laboratory of Numerical Computations, Polytechnic University of Catalonia

[e.g. Khan et al., 2006; Tirone et al., 2009; Herbert et al., 2009; Afonso et al., 2013a;b; Duesteroheft et al., 2014]. Some of the most important advantages of this implementation, commonly known as the "dynamic" approach, are that it is free from P-T-C discretization errors, it allows for a more accurate tracking/modelling of chemical reactions, phase changes, and partitioning of chemical species (e.g. during partial melting and reactive flow) in geodynamic simulations, and it does not require *a priori* estimates of the P-T-C conditions and relevant parameters before the simulation/inversion. The tradeoff is that dynamic implementations are more computationally expensive than static ones; when the number of computations is large, as in high-resolution large-scale thermo-mechanical simulations of mantle convection, this approach can become prohibitively expensive. Also, the presence of first-order phase transformations can cause problems due to numerical singularities arising during the minimization [Connolly, 2009].

Another example of practical importance where both static and dynamic approaches are desirable is geophysical inversions for the physical state of the lithosphere and mantle [e.g. Khan et al., 2006; 2011; Kuskov and Konrod, 2006; Cammarano et al., 2009; 2011; Afonso et al., 2013a,b; Kuskov et al., 2014; Shan et al., 2014; Kaban et al., 2014]. In particular, the method of Afonso et al., [2013a,b] solves a complete energy minimization problem for each mantle node (characterized by a specific T-P-C) of all Earth models tested during the probabilistic inversion (typically of the order of 10^5-10^8). However, since such probabilistic approach requires a thorough exploration of the compositional space and a large number of energy minimization problems, the compositional space has been limited to simple peridotitic compositions within the mantle, leaving the more complicated and heterogeneous crustal component as a parameterized model; this seriously limits the application of probabilistic inversions for the thermochemical structure of the crust.

The increasing interest in implementing thermodynamic phase equilibria information into geophysical and geodynamic problems prompts the following questions: how can a non-specialist easily implement thermodynamic phase equilibria information into her/his geophysical or geodynamic models? what is the most general and efficient way to do it? how can the user control the accuracy of the input thermodynamic information? The first question has been recently addressed by Zunino et al., [2011] and Duesterhoeft and de Capitani [2013], who provided open-source tools that facilitates the implementation of static and dynamic thermodynamic information, respectively. Unfortunately, both tools are built on top of specific energy minimization software and databases, thus somewhat limiting their generality and reach.

In this contribution we address all three questions, with particular emphasis on the last two and focusing on the generality, efficiency, and quality control of the proposed method. By generality we mean that the thermodynamic information can be obtained from *any* thermodynamic modelling program and/or database; i.e. users have total freedom to use their program/database of choice. By efficiency we mean that the method/algorithm must allow the user to be able to store and retrieve the *relevant* thermodynamic information (e.g. density, specific heat, thermal expansion, etc) very efficiently during the simulation/inversion. Finally, quality control refers to the ability to control, efficiently and rigorously, the accuracy or quality of the thermodynamic information needed for the inversion/simulation. This can become important during the preliminary or exploratory stages of a study, where the user may want to compromise accuracy in favour of rapid solutions. We present a general, efficient and easy-to-use algorithm that can be used in both dynamic and static approaches and that overcomes

the limitations of previously proposed adds-on tools (see next section). The algorithm is based on a generalization of the Proper Orthogonal Decomposition method to higher dimensions. Decomposition methods have been extensively used in many different scientific fields. Examples include chemometrics [Henrion et al., 1993, Andersson and Henrion, 1999], linear algebra and numerical analysis [De Lathauwer et al.,2000, Ibraghimov, 2002] and neurosciences [Beckmann and Smith, 2005]. This list is by no means exhaustive. Decomposition techniques, however, have not been yet exploited in the geoscience community.

2. Method

2.1. Separated representation of functions

The data produced by a thermodynamic modeling program is usually output and/or stored as high-dimensional tables containing the properties of interest (e.g. density, heat capacity, etc) as functions of e.g. pressure, temperature, water content, melt depletion degree, composition, etc. The large dimensionality of these tables becomes a problem because the number of coefficients to be stored grow exponentially with the number of dimensions. Therefore, describing a function in D dimensions (e.g. density depending on T, P, etc), requires $n_{full} = \prod_{d=1}^{D} n_d$ coefficients, where n_d is the number of points/nodes used in the discretization of the *d-th* dimension. In practice, one solution to avoid the exponential growth of coefficients is the use of *separable* representations. A function is said to be separable if it has the form,

$$f(x_1, x_2, ..., x_D) = \sum_{m=1}^{M} F_1^m(x_1)F_2^m(x_2)...F_D^m(x_D) = \sum_{m=1}^{M}\prod_{d=1}^{D} F_d^m(x_d),$$
$$(1)$$

that is, f is written as a sum of M terms (or *modes*), and each term is a product of functions depending on one dimension only. The advantage of this form is that the number of coefficients to be stored is now linear with the number of dimensions,

$$n_{sep} = M\sum_{d=1}^{D} n_d. \qquad (2)$$

For example, if $n_1 = n_2 = n_3 = n_4 = 50$, then $n_{full} = 50^4 = 6250000$ while $n_{sep} = 200M$. In most cases, M is a small number (in all the examples presented in this paper $M \lesssim 100$), therefore, the compression of information in the separated representation is extremely high (see examples in Section 3).

The same idea of separability can be extended from multidimensional functions to multidimensional tensors. A separable tensor $\mathcal{S}$ has the form

$$\mathcal{S} = \sum_{m=1}^{M} \mathbf{a}^m \otimes \mathbf{b}^m \otimes \mathbf{c}^m. \qquad (3)$$

where $\mathbf{a}^m$, $\mathbf{b}^m$ and $\mathbf{c}^m$ are vectors and $\otimes$ denotes the standard tensor product. This separation is illustrated for a 3D case in Figure 1. Note that in most cases, $\mathbf{a}^m$, $\mathbf{b}^m$, $\mathbf{c}^m$ can be identified as the discretized versions of the functions F_1^m, F_2^m and F_3^m in equation (1).

Many procedures have been proposed to obtain separated approximations of known functions (continuum space) or tensors (discrete space, e.g. tables). If the number of dimensions is two, the separated approximation can be computed using a Singular Value Decomposition (SVD) or any other related technique. For this case, SVD is said to be optimal in the sense that the separated representation is such that the number of terms required to obtain a given accuracy is lower

than for any other decomposition [*Eckart and Young*, 1936]. Unfortunately, this property is lost for higher dimensions [*Kolda*, 2001]. Consequently, a number of higher-order techniques have been proposed, each with particular advantages and limitations. Some examples are the *Higher-Order SVD* [*De Lathauwer et al.*, 2000], the CANDECOMP/PARAFAC [*Carroll and Chang*, 1970; *Harshman*, 1970] and the Tucker decomposition [*Tucker*, 1966]. An overview of these techniques can be found in *Kolda and Bader* [2009].

For the present purposes, we adopt a version of the CANDECOMP/PARAFAC method based on an alternating linear least-squares algorithm (hereafter, CP ALS). This method is one of the simplest to implement and typically outperforms other methods in obtaining separated representations of thermodynamic functions (see Section 3). Moreover, it is many orders of magnitude faster than the actual generation of the primary thermodynamic data, and therefore it does not add any significant extra computational time. In the next section, we briefly describe the basic idea of the CP ALS algorithm. To simplify the description, we use a three-dimensional table (a cube) as default. The same ideas can be easily extended to any number of dimensions.

2.2. CP ALS algorithm

Relevant notations and definitions related to this section can be found in Appendix A. The general problem to be solved is stated as follows: The full third order ($D = 3$) real-valued tensor $\mathcal{T}$ has dimensions $I \times J \times K$. This tensorial space is denoted as $\mathbb{R}^{I \times J \times K}$, where $I = n_1$, $J = n_2$, $K = n_3$. In the present context, this tensor would represent e.g. a table containing density as a function of P-T-H_2O.

Our goal is to find a separable approximation $\mathcal{S}$ of the tensor $\mathcal{T}$. This representation has the form described in Eq. (3). Therefore, we need to determine the vectors $\mathbf{a}^m$, $\mathbf{b}^m$ and $\mathbf{c}^m$ that compose $\mathcal{S}$. The problem to be solved, then, is find $\mathcal{S}$ such that,

$$\min_{\mathcal{S}} ||\mathcal{T} - \mathcal{S}||. \qquad (4)$$

Arranging the vectors $\mathbf{a}^m$ as columns, a factor matrix $\mathbf{A} = [\mathbf{a}^1 \, \mathbf{a}^2 \, \mathbf{a}^3 \ldots \mathbf{a}^M]$ is defined. Matrices $\mathbf{B}$ and $\mathbf{C}$ are defined similarly.

Problem (4) is nonlinear because the form of the separated function imposes a product of the unknown vectors. The CP ALS algorithm uses an alternating direction scheme to deal with this nonlinearity. First, it fixes $\mathbf{B}$ and $\mathbf{C}$ and solves for $\mathbf{A}$. Then, it fixes $\mathbf{A}$ and $\mathbf{C}$ and solves for $\mathbf{B}$. Finally, it fixes $\mathbf{A}$ and $\mathbf{B}$ and solves for $\mathbf{C}$. These steps are repeated until convergence is achieved. Note that each of these steps only involves solving a linear least-squares problem. At every step, the CP ALS method finds an approximation for all vectors corresponding to one dimension, i.e. a first approximation for all $\mathbf{a}^m$ (the factor matrix $\mathbf{A}$), then for all $\mathbf{b}^m$ (the factor matrix $\mathbf{B}$), etc. This can be done very efficiently by solving a linear system of size $M \times M$, where M is the number of terms in the sum of $\mathcal{S}$ (Eq. 3).

In the standard implementation of the CP ALS algorithm, each of the linear steps assumes that D -1 dimensions are known. For example, the first problem reads: given the full tensor $\mathcal{T}$ and the factor matrices $\mathbf{B}$ and $\mathbf{C}$ (related to the separated form of $\mathcal{S}$), find $\mathbf{A}$ such that

$$\min_{\mathcal{S}} ||\mathcal{T}_{(1)} - \mathcal{S}_{(1)}|| = \min_{\mathcal{S}} ||\mathcal{T}_{(1)} - \mathbf{A}(\mathbf{C} \odot \mathbf{B})^\top||. \qquad (5)$$

Here, $\mathcal{T}$ and $\mathcal{S}$ were replaced by their reshaped versions along the dimension we are solving for, and then $\mathcal{S}_{(1)}$ was written in terms of its factor matrices using the Khatri-Rao product (see Appendix A). Note that after the reshaping operation, the norm in (5) became a standard Frobenius norm. The optimal solution of (5) is given by

$$\mathbf{A} = \mathcal{T}_{(1)} \left[(\mathbf{C} \odot \mathbf{B})^\top \right]^+ . \qquad (6)$$

The Khatri-Rao product can be rewritten as [*Kolda and Bader*, 2009],

$$\mathbf{A} = \mathcal{T}_{(1)}(\mathbf{C} \odot \mathbf{B})(\mathbf{C}^\top \mathbf{C}. * \mathbf{B}^\top \mathbf{B})^{-1}. \qquad (7)$$

which has the advantage of being a square $M \times M$ linear system. The subsequent steps to find $\mathbf{B}$ and $\mathbf{C}$ are essentially the same.

This ends the description of the basic version of the CP ALS algorithm as proposed in *Carroll and Chang* [1970] and *Harshman* [1970]. Improvements to the basic algorithm have been proposed in the literature; relevant examples in the context of chemometrics include *Acar et al.* [2011] and *Kang et al.* [2015]. Moreover, open-source implementations of CP ALS and variations of it are available in several computer languages. Examples include the MATLAB Tensor toolbox by *Bader et al.* [2015] and the FORTRAN Multilinear Engine [*Paatero,*, 1999]. Our particular implementation (included in this submission as supplementary material) is written in MATLAB and tailored to facilitate the incorporation of thermodynamic information from thermodynamic modeling programs into existent inversion and/or geodynamic codes.

One drawback of the CP ALS algorithm is the need to choose the number of terms M for the separated representation before performing the actual decomposition. Since it is difficult to estimate *a priori* the number of terms required to obtain a predefined accuracy, in practice, several trials with different values of M need to be preformed until an appropriate value is found. An alternative is the algorithm proposed in our previous work [*Modesto et al.*, 2015], which enriches the separated solution by sequentially adding terms to the separated solution. In this way, the enrichment can be stopped when a specific accuracy threshold is obtained without the need of restarting the procedure for every value of M. The trade-off of this approach is that it usually produces separated functions having more terms than the CP ALS algorithm. Although the examples shown in this paper have been computed with the CP ALS algorithm, we also provide a MATLAB implementation of the enriched algorithm.

3. Examples

In this section we present some illustrative examples to highlight the advantages and drawbacks of the proposed approach for implementing thermodynamic phase equilibria information into geophysics/geodynamics problems. Although these examples are representative of real applications in geophysics and geodynamics, they are illustrative in nature and should not be taken strictly as final products or implementation recipes.

3.1. Example1: The P-T-H_2O case

This case is typical of large-scale thermomechanical simulations, where different lithologies are used to model distinct lithospheric bodies and no reactions or diffusion between these domains is allowed other than hydration/dehydration reactions (e.g. Gerya et al., 2006; Yamato et al., 2007; Nikolaeva et al., 2008; Hebert et al., 2009; Afonso and Zlotnik, 2011). As a practical example, we choose a peridotitic composition and discretize our P-T-H_2O space as follows: 400 nodes for the P-axis in the range $0 < P < 15$ GPa, 400 nodes for the T-axis in the range $273 < T < 2000$ K, and 5 nodes for the water axis with constant contents of 0, 1, 2, 3, and 4%. This discretization thus amounts to 8×10^5 values

to be stored *per parameter of interest* (e.g. density, Cp, coefficient of thermal expansion, etc).

We solve the energy minimization problem with the software Perple_X [Connolly, 2009] using the thermodynamic database of Holland and Powell [2011]. We then post-process this primary information with CP ALS to obtain a compact representation of the results. The first row in Fig. 2 shows the density fields obtained from the minimization problem as functions of P-T for all five cases with different water contents. The second and third rows in Fig. 2 show, respectively, the same density fields given by the CP ALS algorithm with 100 terms and the difference between the two solutions. Figure 3 shows a comparison of the full solution with different separated solutions using 10, 40 and 100 terms. One can see that even in the case with 40 terms, it is difficult to perceive any difference between the full and CP ALS results. The mean error associated with the lowest resolution is $< 0.14\%$, demonstrating that our separated representation can reproduce the relevant information accurately, even with a small number of terms. This mean error becomes an order of magnitude smaller in the cases with 40 and 100 terms (Table 1). We also see that the rate of error reduction (i.e. increase in the explained variance) is more dramatic within the first 30-40 terms, and it becomes less pronounced for higher terms.

The compression ratio achieved by the separated solution can be defined as

$$\mathrm{CR} = 100 - \frac{\mathrm{SV}_{sep}}{\mathrm{SV}_{full}} \times 100 \qquad (8)$$

where SV_{sep} and SV_{full} are the stored values in memory needed by the separated solution and those given by the full table, respectively. We therefore see that the compression ratio of the lowest resolution case is a staggering $\sim 99\%$ (Table 1). In other words, to reproduce the relevant information (bulk density, in this case) with a mean error of $\sim 0.14\%$ within the entire P-T space, we only need to store $\sim 1\%$ of the original information (i.e. only 8050 coefficients). Even in the case with 40 terms, the compression ratio is $\sim 96\%$ (Table 1).

As expected, the main sources of error are related to regions with sharp discontinuities in the fields (e.g. major phase transitions), as the decomposition algorithm tends to smooth sharp gradients (Figs. 2, 4). We can partially alleviate this problem by adding more terms (i.e. higher frequencies). However, this prompts the question of how critical and representative these errors really are. The location of major phase transitions predicted by internally-consistent databases are affected by uncertainties that, although difficult to estimate and rarely reported, should be in the range of tens to hundreds of MPa and tens of °C [e.g. Chatterjee et al., 1998]. The errors in the solutions from our algorithm are directly associated to the impossibility of CP to reproduce the exact position and sharpness of the transition as predicted by the database (Fig. 4). However, when we consider the uncertainties associated with the actual prediction of the phase transition, the computational error arising from our algorithm becomes immaterial for all practical purposes.

3.2. Example 2: The F-P-T-H_2O case

Another case of practical interest is the tracking of a partial melting path for mantle rocks with different water contents. This scenario may be relevant e.g. for the simulation of mantle wedge dynamics [e.g. Sobolev and Babeyko, 2005; Faccenda et al., 2008; Nikolaeva et al., 2009; Gerya, 2011; Duesteroheft et al., 2014] and lithospheric mantle stability [e.g. Hirth and Kohlstedt, 1996; Li et al., 2008; Wang et al., 2014], where the thermophysical properties of the solid residue (i.e. mantle rocks) changes continuously as melting proceeds, therefore affecting the dynamic evolution of the

simulation. In terms of computing the necessary thermodynamic phase equilibria information, we just need to add an extra axis with the melt fraction F. Each value of F thus corresponds to a specific solid residue composition given by the chosen melting model. For illustration purposes, we use the polybaric perfect-fractional melting model of Herzberg [2004].

For this example, we use a discretization representative of those used in large-scale geodynamic models [e.g. Nakagawa et al., 2010; Afonso and Zlotnik, 2011]. Pressure is discretized with 501 nodes ($\Delta P \sim 180$ MPa), temperature with 151 nodes ($\Delta T \sim 8$ °C), and water content with 5 nodes ($\Delta H_2O = 1\%$wt, as in the previous example). The F-axis is discretized with 6 nodes with constant melt values of 0, 1, 2, 3, 4 and 5% melt (i.e. 6 distinct solid residue compositions). This gives a total of $> 1.89 \times 10^6$ individual nodes *for each* physical parameter of interest.

Statistics for the 4D separated representation of bulk density are listed in Table 1. Including 50 terms in the separated solution results in a maximum (local) error of 1.62% (again, only at the locus of sharp phase transitions). The corresponding mean error, however, is as low as 0.02%, indicating that the separated representation is an excellent description of the field. Note also that the compression achieved in this case is $> 98\%$ (i.e. only 1.46% of the full table), significantly higher than in the equivalent representation of the 3D case described in the previous section ($\sim 95\%$ for 50 terms). This is a typical trend in high-dimensional problems, where the compression ratio becomes more substantial as the number of dimensions increase.

Another important feature of the proposed method is that the finer the discretization of the axes, the larger the compression achieved by the separated representation. For instance, although the use of a 6 node grid for melt fraction (steps of 1%) is practical given common memory requirements during large-scale thermomechanical simulations, large interpolation errors are expected at midpoint melt fraction values. The use of finer grids in pre-computed tables, on the other hand, may become unfeasible if a significant number of lithologies are to be used (and stored in memory) in a simulation. The staggering compression provided by the separated representation, however, overcomes this limitation and allows the use of much finer grids. To illustrate this, let us rediscretize the F-P-T-H_2O example above, keeping the same discretization for P and T, but increasing the discretization of F and H_2O to 51 and 17 nodes, respectively (i.e. $\Delta F = 0.005\%$ and $\Delta H_2O = 0.25\%$wt). The full table now contains $> 65.5 \times 10^6$ coefficients. The separated solution with 50 terms has an average error of 0.02%, a maximum (localized) error of 1.88% and allows a massive compression of 99.95% (only 0.05% of coefficients are stored with respect with the full table). This compression reduces the memory requirement to that of an equivalent full 4D table with only ~ 14 nodes per dimension. Such drastic reduction in memory requirements makes it possible to work with much finer discretizations and thus significantly reduce interpolation errors in numerical simulations and inversions.

4. Conclusions and Final Remarks

We have presented a flexible, general and efficient approach, based on a generalization of the Proper Orthogonal Decomposition method, that facilitates the implementation of thermodynamic phase equilibria information into a wide range of geophysical and geodynamic studies. The main virtues of the present approach can be summarized as follows:

• The method is easy to implement in any scientific language. As such, it can be incorporated into existing geodynamic/geophysical codes or used as a separate pre-processing software.

• The method is independent of particular thermodynamic software or databases. Users can use any software or database to create the desired primary thermodynamic information encoded in multi-dimensional tables.

• The amount of stored information required by the proposed method to reproduce the original information to a high level of accuracy is typically of the order of 1-5% of the original information. This drastic compression of information allows using much finer P-T-C grids, therefore minimizing discretization errors. It also largely overcomes the so-called "curse of dimensionality" affecting other standard methods, allowing the use of significantly larger thermodynamic datasets (e.g. more lithologies, melting paths, etc) than otherwise possible with raw pre-computed tables.

• The method permits an easy characterization and control of the errors associated with the separated representation of thermodynamic data. This is important when working with preliminary models/inversions, where accuracy can be compromised in favour of computational speed. Moreover, smoothing errors associated with the separated representation are only significant at the locus of large discontinuities (i.e. phase transitions). These errors, however, are either smaller or comparable to those already present in the original thermodynamic data.

Although not discussed in this contribution, derivatives of the fields (e.g. $\partial Vs/\partial T$) are easily and directly obtained from the separated solution [e.g. Zlotnik et al, 2015]. This can be particularly useful e.g. when working with matrix-based inversions method, where the matrices of partial derivatives are needed.

A shortcoming of the described approach is related to the fact that we still need to compute the primary thermodynamic information, so we can then decompose it *a posteriori* to generate the separated solution. In reality, this can be also viewed as and advantage, as it allows the user to have a better control on the actual primary information to be used in her/his simulations or inversions. Also, this primary information can be saved in a "library" and used in subsequent studies. However, we expect that the extension of *a posteriori* decomposition methods, such as the one described here, to truly Proper Generalised Decomposition solutions [e.g. Ammar et al, 2010, Zlotnik et al, 2015] for the free energy minimization problem would bring important additional benefits to the "on-the-fly" or dynamic implementation of thermodynamic information into geophysical and geodynamic investigations. We are currently working on this.

Appendix A: Notation and definitions

Vectors are denoted by boldface lowercase letters (e.g. **a**), matrices as boldface capital letters (e.g. **A**) and tensors by boldface script letters (e.g. $\mathcal{A}$).

The norm of a tensor $\mathcal{T} \in \mathbb{R}^{I \times J \times K}$, is the trivial extension of the Frobenius norm for matrices:

$$||\mathcal{T}|| = \sqrt{\sum_{i=1}^{I} \sum_{j=1}^{J} \sum_{k=1}^{K} t_{ijk}^2}.$$

One operation that facilitates notation and, in addition, gives some clues on the implementation, is the *reshape* operation (also known as *matricization* or *unfolding* or *flattening*). The reshape operation converts a n-dimensional tensor into a matrix (second order tensor). It can be performed along any dimension d of the tensor: the columns of the resulting matrix are taken as the values of the tensor along the dimension d. If $\mathcal{T} \in \mathbb{R}^{I \times J \times K}$ then the size of the three possible reshapes are $\mathcal{T}_{(1)} \in \mathbb{R}^{I \times JK}$, $\mathcal{T}_{(2)} \in \mathbb{R}^{J \times IK}$ and $\mathcal{T}_{(3)} \in \mathbb{R}^{K \times IJ}$. The next example illustrates this operation:

let $\mathcal{T} \in \mathbb{R}^{2 \times 3 \times 2}$ defined by its two frontal slices:

$$\mathcal{T}(:,:,1) = \begin{bmatrix} 1 & 3 & 5 \\ 2 & 4 & 6 \end{bmatrix} \quad \text{and} \quad \mathcal{T}(:,:,2) = \begin{bmatrix} 7 & 9 & 11 \\ 8 & 10 & 12 \end{bmatrix}$$

then, the three reshape operations are

$$\mathcal{T}_{(1)} = \begin{bmatrix} 1 & 3 & 5 & 7 & 9 & 11 \\ 2 & 4 & 6 & 8 & 10 & 12 \end{bmatrix}, \quad \mathcal{T}_{(2)} = \begin{bmatrix} 1 & 2 & 7 & 8 \\ 3 & 4 & 9 & 10 \\ 5 & 6 & 11 & 12 \end{bmatrix} \quad \text{and } \mathcal{T}_{(3)} = \begin{bmatrix} 1 & \\ 7 & \end{bmatrix}$$

The tensor product $\otimes$ produce a tensor $\mathcal{T}$ in which each element or the tensor is the product of the corresponding vector elements, for example, $\mathcal{T} = \mathbf{a} \otimes \mathbf{b} \otimes \mathbf{c}$ produce $t_{ijk} = a_i b_j c_k$.

Two special matrix products are required. The first one is called the *Hadamard* product denoted by $.*$ and consisting of the elementwise matrix multiplication. Given $\mathbf{A} \in \mathbb{R}^{I \times J}$ and $\mathbf{B} \in \mathbb{R}^{I \times J}$ their Hadamard product is

$$\mathbf{A}.*\mathbf{B} = \begin{bmatrix} a_{11}b_{11} & a_{12}b_{12} & \dots & a_{1J}b_{1J} \\ a_{21}b_{21} & a_{22}b_{22} & \dots & a_{2J}b_{2J} \\ \vdots & & \ddots & \vdots \\ a_{I1}b_{I1} & a_{I2}b_{I2} & \dots & a_{IJ}b_{IJ} \end{bmatrix}.$$

The second product is the so-called *Khatri-Rao* product denoted by $\odot$. Given $\mathbf{A} \in \mathbb{R}^{I \times R}$ and $\mathbf{B} \in \mathbb{R}^{J \times R}$ then $\mathbf{A} \odot \mathbf{B} \in \mathbb{R}^{IJ \times R}$ is defined as

$$\mathbf{A} \odot \mathbf{B} = \begin{bmatrix} \mathbf{a}_1 \otimes \mathbf{b}_1 & \mathbf{a}_2 \otimes \mathbf{b}_2 & \dots & \mathbf{a}_R \otimes \mathbf{b}_R \end{bmatrix}.$$

Finally, the Moore-Penrose pseudoinverse of a matrix is a generalization of the inverse of matrix applicable to non-square matrices [*Penrose*, 1955]. The pseudoinverse of the matrix $\mathbf{A}$ is denoted by $\mathbf{A}^+$.

Table 1. Top: Results of the separation the 3D table P-T-H_2O (Example 1) for different number of terms (number of coefficients of the full tensor $n_{full} \approx 8.0 \times 10^5$ per parameter of interest). Bottom: Results of the separation the 4D table F-P-T-H_2O with different number of terms (number of coefficients of the full tensor $n_{full} \approx 65.59 \times 10^6$). NCE: number of coefficients having error larger than 1%. n_{sep} number of coefficient stored in the separated representation. CR: compression ratio computed as described in the text.

| Terms	Max err.	Mean err.	NCE	n_{sep}	CR
10	3.70%	0.14%	8767	8050	98.9%
20	2.93%	0.08%	2295	16100	97.9%
30	2.30%	0.06%	1005	24150	96.9%
40	1.94%	0.05%	553	32200	95.9%
50	1.90%	0.04%	313	40250	94.9%
60	1.90%	0.04%	163	48300	93.9%
70	1.82%	0.03%	127	56350	92.9%
80	1.78%	0.03%	78	64400	91.9%
90	1.66%	0.03%	49	72450	90.9%
100	1.69%	0.03%	43	80500	89.9%
10	4.27%	0.07%	10291	6630	0.29%
20	3.02%	0.05%	3837	13260	0.58%
30	2.53%	0.04%	1961	19890	0.88%
40	2.09%	0.03%	1294	26520	1.17%
50	1.62%	0.02%	281	33150	1.46%

References

Acar, E., D. M. Dunlavy, and T. G. Kolda (2011), A scalable optimization approach for fitting canonical tensor decompositions, *Journal of Chemometrics*, *25*(2), 67–86.

Afonso, J. C., Fernàndez, M., Ranalli, G., Griffin, W.L. and J.A.D. Connolly (2008), Integrated geophysical-petrological modelling of the lithospheric-sublithospheric upper mantle: methodology and applications. *Geochem. Geophys. Geosyst.* 9, Q05008, doi:10.1029/2007GC001834.

Afonso, J.C. and D. Schutt (2012), The effects of polybaric partial melting on the density and seismic velocities of mantle restites, *Lithos*, 134-135, 289-303.

Afonso, J. C., J. Fullea, W. L. Griffin, Y. Yang, A. G. Jones, J. A. D. Connolly, and S. Y. O'Reilly (2013a), 3-D multi-observable probabilistic inversion for the compositional and thermal structure of the lithosphere and upper mantle. I: A priori petrological information and geophysical observables, J. Geophys. Res. Solid Earth, 118, 25862617, doi:10.1002/jgrb.50124

Afonso, J. C., J. Fullea, Y. Yang, J. A. D. Connolly, and A. G. Jones (2013b), 3-D multi-observable probabilistic inversion for the compositional and thermal structure of the lithosphere and upper mantle. II: General methodology and resolution analysis, J. Geophys. Res. Solid Earth, 118, 16501676, doi:10.1002/jgrb.50123

Ammar, A.,Chinesta, F. Díez, P. and Huerta, A., (2010), An error estimator for separated representations of highly multidimensional models, Computer Methods in Applied Mechanics and Engineering, 199, 25-28, 1872–1880.

Andersson C. A. and Henrion R., A general algorithm for obtaining simple structure of core arrays in N-way PCA with application to fluorimetric data, Computational Statistics & Data Analysis, 31 (1999), pp. 255?278.

Bader, B. W., T. G. Kolda, et al. (2015), Matlab tensor toolbox version 2.6, http://www.sandia.gov/ tgkolda/TensorToolbox/.

Beckmann C. and Smith.S. (2005), Tensorial extensions of independent component analysis for multisubject FMRI analysis, NeuroImage, 25 (2005), pp. 294?311.

Cammarano F., Tackley P. and L. Boschi (2011), Seismic, petrological and geodynamical constraints on thermal and compositional structure of the upper mantle: global thermo-chemical models, Geophys. J. Int., 187, 1301-1318.

Carroll, J. D., and J.-J. Chang (1970), Analysis of individual differences in multidimensional scaling via an n-way generalization of "Eckart-Young" decomposition, *Psychometrika*, *35*(3), 283–319.

Chatterjee, N.D., Kruger, R., Haller, G., Olbricht, W., (1998), The Bayesian approach to an internally consistent thermodynamic database: theory, database and generation of phase diagrams, Contrib. Min. Petrol., 133, 149-168.

Connolly, J.A.D. (2009), The geodynamic equation of state: what and how, Geochem. Geophys. Geosys.,10, Q10014, doi:10.1029/2009GC002540.

De Lathauwer, L., B. De Moor, and J. Vandewalle (2000), A multilinear singular value decomposition, *SIAM J. Matrix Anal. Appl.*, *21*(4), 1253–1278.

Davies, D. R., Goes, S., Davies, J.H., Schuberth, B.S.A., Bunge, H-P., Ritsema, J. (2012), Reconciling dynamic and seismic models of the Earth's lower mantle: The dominant role of thermal heterogeneity. Earth Planet. Sci. Lett., 353-354, 253-269.

Eckart, C., and G. Young (1936), The approximation of one matrix by another of lower rank, *Psychometrika*, *1*(3), 211–218, doi: 10.1007/BF02288367.

Ibraghimov I., Applicationofthethree-waydecompositionformatrixcompression,Numerical Linear Algebra with Applications, 9 (2002), pp. 551?565.

Ganguly, J., Freed, A.M., Saxena, S.K. (2009), Density profiles of oceanic slabs and surrounding mantle: Integrated thermodynamic and thermal modeling, and implications for the fate of slabs at the 660km discontinuity. Phys. Earth Planet. Int., 172, 257-267.

Harshman, R. A. (1970), Foundations of the PARAFAC procedure: Models and conditions for an "explanatory" multimodal factor analysis, *UCLA working papers in phonetics*, *16*, 1–84.

Herzberg, C. (2004), Geodynamic information in peridotite petrology. *J. Petrol.*, 45, 2507-2530.

Hirth, G., and D. L. Kohlstedt, Water in the oceanic upper mantle: implications for rheology, melt extraction and the evolution of the lithosphere, *Earth Planet. Sci. Lett.*, *144*, 93–108, 1996.

Holland, T. J. B. and Powell, R. (2011), An improved and extended internally consistent thermodynamic dataset for phases of petrological interest, involving a new equation of state for solids. Journal of Metamorphic Geology, 29: 333383. doi: 10.1111/j.1525-1314.2010.00923.x

Kaban, M. K., M. Tesauro, W. D. Mooney, and S. A. P. L. Cloetingh (2014), Density, temperature, and composition of the North American lithosphereNew insights from a joint analysis of seismic, gravity, and mineral physics data: 1. Density structure of the crust and upper mantle, Geochem. Geophys. Geosyst., 15, 47814807, doi:10.1002/2014GC005483.

Kang, C., H.-L. Wu, J.-J. Song, H. Xu, Y.-J. Liu, Y.-J. Yu, X.-H. Zhang, and R.-Q. Yu (2015), A flexible trilinear decomposition algorithm for three-way calibration based on the trilinear component model and a theoretical extension of the algorithm to the multilinear component model, *Analytica Chimica Acta*, *878*, 63 – 77, doi: 10.1016/j.aca.2015.03.034.

Khan, A., L. Boschi, and J. A. D. Connolly (2011), Mapping the Earth's thermochemical and anisotropic structure using global surface wave data, J. Geophys. Res., 116, B01301, doi:10.1029/2010JB007828.

Kolda, T. G. (2001), Orthogonal tensor decompositions, *SIAM Journal on Matrix Analysis and Applications*, *23*(1), 243–255.

Kolda, T. G., and B. W. Bader (2009), Tensor decompositions and applications, *SIAM Rev.*, *51*(3), 455–500.

Kuskov, O. L., Kronrod, V.A. and A.A. Prokofev (2011), Thermal structure and thickness of the lithospheric mantle underlying the Siberian Craton from the Kraton and Kimberlite superlong seismic profiles, Izvestiya, Physics of the Solid Earth, 47, 155175.

Kuskov, O. L., V. A. Kronrod, and N. I. Pavlenkova. (2014) Thermodynamic-Geophysical Modeling of the Interior Structure of the Siberian Cratonic Mantle along Cross-Cutting Profiles Kimberlite and Meteorite. J Geol Geosci., 3, 155, 2.

Modesto, D., S. Zlotnik, and A. Huerta (2015), Proper Generalized Decomposition for parameterized helmholtz problems in heterogeneous and unbounded domains: application to harbor agitation, *Comput. Methods Appl. Mech. Eng.*, accepted for publication.

Paatero., P. (1999), The multilinear engine: a table-driven, least squares program for solving multilinear problems, including the n-way parallel factor analysis model, *Journal of Computational and Graphical Statistics*, *8*(4), 854–888, doi: 10.1080/10618600.1999.10474853.

Penrose, R. (1955), A Generalized Inverse for Matrices, *Proc. Cambridge Phil. Soc.*, *51*, 406–413.

Tucker, L. R. (1966), Some mathematical notes on three-mode factor analysis, *Psychometrika*, *31*, 279–311.

Nakagawa, T., Tackley, P.J., Deschamps, F., Connolly, J.A.D. (2010), The influence of MORB and harzburgite composition on thermo-chemical mantle convection in a 3D spherical shell with self-consistent calculated mineral physics. Earth Planet. Sci. Lett., 296, 403-412.

Shan, B., J. C. Afonso, Y. Yang, C. J. Grose, Y. Zheng, X. Xiong, and L. Zhou (2014), The thermochemical structure of the lithosphere and upper mantle beneath south China: Results from multiobservable probabilistic inversion, J. Geophys. Res. Solid Earth, 119, 84178441, doi:10.1002/2014JB011412.

Stixrude, L. and C. Lithgow-Bertelloni (2011), Thermodynamics of mantle minerals II. Phase equilibria, Geophys. J. Int., 184, 11801213, doi: 10.1111/j.1365-246X.2010.04890.x.

Stixrude, L. and C. Lithgow-Bertelloni, Thermodynamics of mantle minerals: 1. Physical properties, Geophysical Journal International, 162, 610-632, 2005, doi: 10.1111/j.1365-246X.2005.02642.x

Vozar, J., A. G. Jones, J. Fullea, M. R. Agius, S. Lebedev, F. Le Pape, and W. Wei (2014), Integrated geophysical-petrological modeling of lithosphere-asthenosphere boundary in central Tibet using electromagnetic and seismic data, Geochem. Geophys. Geosyst., 15, 39653988, doi:10.1002/2014GC005365.

Xu, W., C. Lithgow-Bertelloni, L. Stixrude, and J. Ritsema (2008), The effect of bulk composition and temperature on mantle seismic structure, Earth Planet. Sci. Lett., 275, 70-79, doi:10.1016/j.epsl.2008.08.012.

Zlotnik S., P. Dez, D. Modesto and A,Huerta (2015), Proper generalized decomposition of a geometrically parametrizedheat problem with geophysical applications, J. Numer. Meth. Engng. DOI: 10.1002/nme.4909
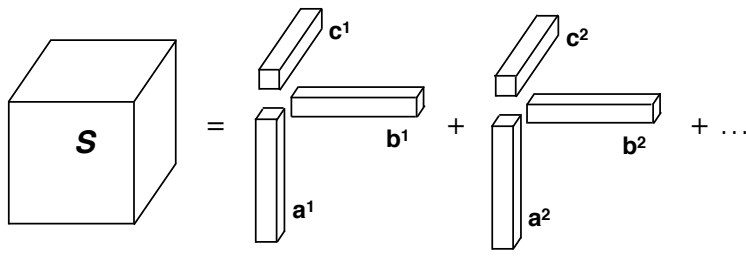
Figure 1. Illustration of the decomposition of a three-dimensional tensor.
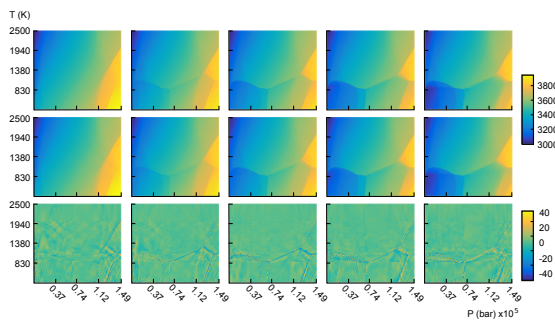

Figure 2. Density fields obtained from the energy minimization problem for water contents from 0 to 4% (from left to right) are shown in the first row. Same fields provided by the CP ALS procedure with 100 terms are shown in the second row. Their absolute difference (full - separated) is shown in the third row.
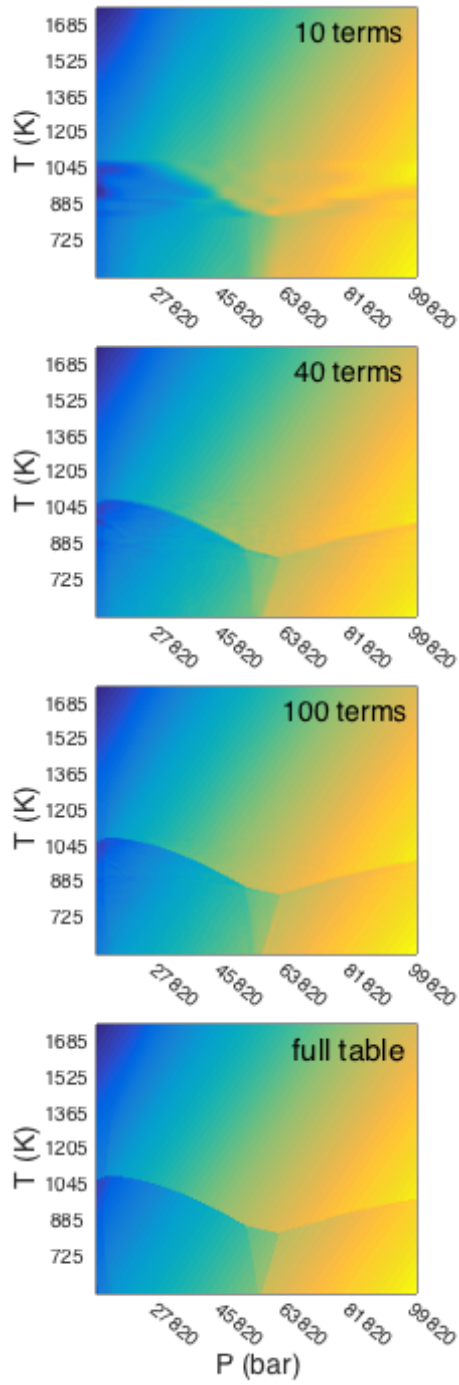
Figure 3. Density fields given by the separated solution with 10, 40 and 100 terms. Only the slice corresponding to F=0%, H_2O=1% is shown.
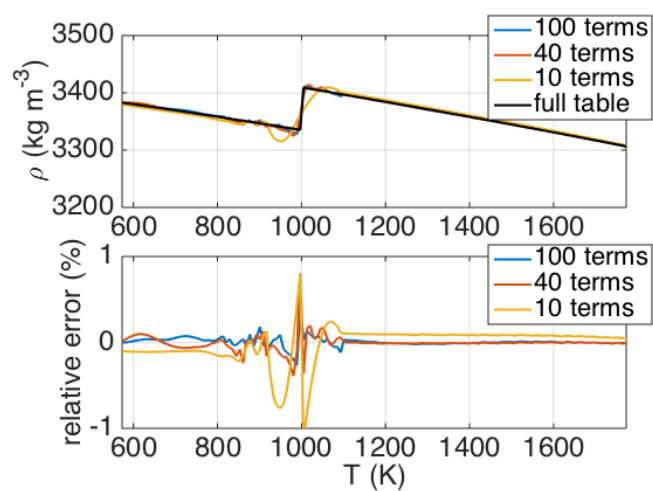
Figure 4. 1D transects through the 3D cube of Example 1 across a major density discontinuity. Note the good representation of the separated solution for terms $\gtrsim 40$